

Critical Exponents of the Three Dimensional Random Field Ising Model

H. Rieger* and A. Peter Young

*Physics Department
University of California
Santa Cruz, CA 95064*

The phase transition of the three-dimensional random field Ising model with a discrete ($\pm h$) field distribution is investigated by extensive Monte Carlo simulations. Values of the critical exponents for the correlation length, specific heat, susceptibility, disconnected susceptibility and magnetization are determined simultaneously via finite size scaling. While the exponents for the magnetization and disconnected susceptibility are consistent with a first order transition, the specific heat appears to saturate indicating no latent heat. Sample to sample fluctuations of the susceptibility are consistent with the droplet picture for the transition.

PACS numbers: 75.10.H, 05.50, 64.60.C.

Submitted to *Europhysics Letters*

Typeset Using *REVTEX*

*Present address: Institut für Theoretische Physik, Universität zu Köln,
5000 Köln 41, Germany.

The three dimensional ferromagnetic Ising model with a random field (RFIM) shows a phase transition to long range order at a critical temperature for small enough field strength [1]. However, the nature of this transition is still unclear; even the question of whether it is first [2] or second [3,4] order remains unsettled. The droplet theory of Villain [5] and Fisher [6] (see also Bray and Moore [7]) develops a self-consistent picture of the transition as well as a set of scaling relations among the critical exponents. Existing numerical studies have been unable to test the validity of these scaling relations because not all the exponents were calculated for any of the relations. The aim of this paper is to determine all critical exponents within a single numerical simulation in order to test the scaling relations predicted by the droplet picture.

The droplet picture makes other predictions which are relevant to our simulations. One is that at and below the transition temperature T_c , the susceptibility is expected to have large sample to sample fluctuations [9]. We therefore need to average over a large number of samples to get a good statistics. Another prediction is thermally activated dynamical scaling [6,5] resulting in a dramatic slowing down in the critical region. This means very long equilibration times. For these reasons we had to confine ourself to modest lattice sizes and the critical exponents will be obtained via finite size scaling.

The Hamiltonian of the system is given by

$$\mathcal{H} = - \sum_{\langle ij \rangle} S_i S_j - \sum_i h_i S_i , \quad (1)$$

where $S_i = \pm 1$ are Ising spins and the first sum runs over all nearest neighbor pairs on an $L \times L \times L$ simple cubic lattice with periodic boundary conditions. The random fields h_i in the second sum, running over all sites, take random values with the discrete probability distribution

$$P(h_i) = \frac{1}{2} \delta(h_i - h_r) + \frac{1}{2} \delta(h_i + h_r) . \quad (2)$$

The Monte Carlo (MC) simulations were performed on a transputer array using 40 T414 transputers. We were able to obtain high performance by using a multi-spin coding algorithm described in [10] in which each transputer simulates 32 physically different systems in parallel, each with a different random field realization. This is somewhat different from

the implementation of multi-spin coding which was applied to the RFIM in [11]. For each run at fixed temperature, T , and field–strength, h_r , we performed a disorder average over 1280 samples. An average over such a large number of samples is necessary because the susceptibility is highly non self–averaging, as mentioned before. The simulations were done for fixed ratio h_r/T at different temperatures.

To check equilibration we simulated two replicas of the system: one starting from an initial configuration with all spins up and one with all spins down. We assumed that the system has reached equilibrium when the magnetization measured for both replicas is the same (within the errorbars). The time needed for equilibration of all 1280 systems varied much with the system size and temperature — in case of the largest size ($L = 16$) we used up to $0.5 \cdot 10^6$ MC–steps for equilibration and $1.5 \cdot 10^6$ MC–steps for measurements. All of the samples were equilibrated for $L < 10$. For larger sizes the number of nonequilibrated samples generally varied between 1% and 3%. The contribution of these samples was estimated to be less than the error bars in the points so so no significant error was made by including them. The only exception to this was for $L = 16, h_r/T = 0.5$ for which 5% of the samples were not equilibrated which gave a significant error in the susceptibility, though not for the other quantities. We therefore ignored this data point when analyzing the susceptibility.

For each sample and each replica (a, b) we recorded the average magnetization per spin $\langle M_{a,b} \rangle$, its square $\langle M_{a,b}^2 \rangle$, the average energy per spin $\langle E_{a,b} \rangle$ and its square $\langle E_{a,b}^2 \rangle$. The angular brackets, $\langle \dots \rangle$, denote a thermal average for a single random field configuration. From these data we get the specific heat per spin, C , the susceptibility χ , the disconnected susceptibility, χ_{dis} , and the order parameter, m , as follows:

$$\begin{aligned} [C]_{\text{av}} &= N \left\{ [\langle E^2 \rangle]_{\text{av}} - [\langle E \rangle^2]_{\text{av}} \right\} / T^2, & [m]_{\text{av}} &= [|\langle M \rangle|]_{\text{av}}, \\ [\chi]_{\text{av}} &= N \left\{ [\langle M^2 \rangle]_{\text{av}} - [\langle M \rangle^2]_{\text{av}} \right\} / T, & [\chi_{\text{dis}}]_{\text{av}} &= N [\langle M \rangle^2]_{\text{av}}, \end{aligned} \tag{3}$$

where $[\dots]_{\text{av}}$ denotes the average over different random field configurations.

The procedure we used to extract the critical exponents is the following: Let $t = T - T_c$ (the deviation from the critical temperature), then the finite size scaling functions for the above quantities read:

$$\begin{aligned}
T^2[C]_{\text{av}} &= L^{\alpha/\nu} \tilde{C}(tL^{1/\nu}), & [m]_{\text{av}} &= L^{-\beta/\nu} \tilde{m}(tL^{1/\nu}), \\
T[\chi]_{\text{av}} &= L^{2-\eta} \tilde{\chi}(tL^{1/\nu}), & [\chi_{\text{dis}}]_{\text{av}} &= L^{4-\bar{\eta}} \tilde{\chi}_{\text{dis}}(tL^{1/\nu}),
\end{aligned}
\tag{4}$$

where α is the specific heat exponent, β the order parameter exponent, ν the correlation length exponent and η and $\bar{\eta}$ describe the power law decay of the connected and disconnected correlation functions, see e.g. [1]. Note that the susceptibility exponent is given by $\gamma = (2 - \eta)\nu$. The scaling function $\tilde{C}(x)$ has a maximum at some value $x = x^*$. For each lattice-size we estimate the temperature $T^*(L)$, where $T^2[C]_{\text{av}}$ is maximal. Since $t^*(L) L^{1/\nu} = x^*$ we obtain in this way the critical temperature T_c and the correlation length exponent ν from:

$$t^*(L) \equiv T^*(L) - T_c = x^* L^{-1/\nu} . \tag{5}$$

We denote the value of $T^*(L)^2 C$ at this temperature $T^*(L)$ by C^* and similarly for the other quantities in Eq. (4). In the vicinity of x^* the scaling function $\tilde{C}(x)$ can be approximated by a parabola. Therefore three temperatures near the maximum of the specific heat are enough to determine the values of $T^*(L)$ as well as $[C^*]_{\text{av}}$ etc. Our results for the exponents obtained in this way are summarized in Table 1. For illustration, we show the results for $T^*(L)$, $[C^*]_{\text{av}}$, $[\chi^*]_{\text{av}}$, $[m^*]_{\text{av}}$ and $[\chi_{\text{dis}}^*]_{\text{av}}$ for $h_r/T = 0.35$ in Fig. 1a–d. Several comments have to be made:

1) The higher the field strength the harder it is to equilibrate the samples. However, the lower the field the less pronounced is the random field behavior for small lattice sizes because of crossover from pure Ising model behavior. Therefore the investigation of larger as well as smaller ratios h_r/T did not seem to be advisable to us. If the transition is of second order and no tricritical point occurs along the critical line (T_c, h_c) the exponents should be universal, i.e. independent of the value of h_r/T .

2) The shift of $T^*(L)$ with respect to T_c becomes smaller for low field strength, so it is harder to determine the exponent ν . In case of $h_r/T = 0.25$ it was not possible to perform an acceptable fit for $T^*(L)$ according to equation (5). The values of ν obtained for the other ratios h_r/T are somewhat higher than that obtained in [4], where $\nu = 1.0 \pm 0.1$.

3) We did not find any indication of a divergence, even logarithmic, of the specific heat, so α is negative. This is different from what is found experimentally [1,8], where the specific heat diverges logarithmically, corresponding to $\alpha = 0$. Furthermore, in our

simulations α seems to get more negative with increasing ratio h_r/T . This may indicate that it is difficult to determine α when α is negative because non-singular (but temperature dependent) background terms can give a significant contribution to the specific heat.

4) The order parameter $[m^*]_{\text{av}}$ shows only a very small size dependence, and does not approach zero but $\lim_{L \rightarrow \infty} [m^*]_{\text{av}} \approx 0.52, 0.50$ and 0.47 for $h_r/T = 0.5, 0.35$ and 0.25 , respectively (see the inset of fig. 1d). This indicates that $\beta = 0$ and that the transition is first order. This seems to contradict our results for the specific heat since the specific heat is expected to diverge as L^d [13] at a first order transition, because of the latent heat, whereas our specific heat data seem to saturate for large L . Perhaps the coefficient of L^d is zero (though we see no symmetry reason for this) or is so small that L^d behavior would only be seen for larger sizes.

5) For the exponent η we get a best estimate that is slightly higher than $1/2$, which is the value obtained below T_c and also the value *at* T_c if the transition is first order [9]. However, the value $\eta = 0.5$ is not excluded by our data. For $h_r/T = 0.5$ we had to exclude the size $L = 16$ from the analysis since 5% of our samples were not equilibrated and the contribution of these samples was larger than the error bars. Our estimates for η are consistent with that obtained in [3]: $\eta = 0.5 \pm 0.1$.

6) The exponent $\bar{\eta}$ for the disconnected susceptibility turns out to be equal to one, so that the scaling relation

$$\beta = (d - 4 + \bar{\eta})\nu/2 \tag{6}$$

is fulfilled (as indicated in the table). We also see that the Schwartz–Soffer [12] inequality

$$\bar{\eta} \leq 2\eta, \tag{7}$$

holds as an equality within the error bars. In [4] it was found that $\bar{\eta} = 1.1 \pm 0.1$.

7) In the droplet picture [5,6] $\theta = 2 - \bar{\eta} + \eta$ is called the violation of hyperscaling exponent. The hyperscaling relations then have the spatial dimension, d , replaced by $d - \theta$, e.g.

$$2 - \alpha = (d - \theta)\nu. \tag{8}$$

As indicated in the table this equality seems *not* to be fulfilled though the error bars are quite large and our estimate for α might be affected by temperature dependent background

terms, as discussed above. The estimates of both sides of this equation cannot be made without knowing *both* α and ν but for $h_r/T = 0.25$ we only determined the ratio. The entries in the table for $2 - \alpha$ and $(d - \theta)\nu$ are therefore left blank for $h_r/T = 0.25$.

8) One of the main predictions of the droplet picture [5,6] is a long tail in the distribution of the susceptibility χ for samples of size L at $T = T_c$ [9]. An analysis of this distribution extracted from our results for the 1280 samples confirms the existence of this long tail. Figure 2 shows the histograms for the probability distribution $P(\chi)$ close to the temperature T^* ($T=3.80$ for $L=8$ and $T=3.75$ for $L=16$) for $h_r/T=0.35$. The second moment of this distribution $[\chi^{*2}]_{av}$, shown in the inset of fig. 1c, scales like L^ζ , with $\zeta = 3.8 \pm 0.1$ (for $h_r/T = 0.35$), which is larger than the square of the mean $L^{4-2\eta} \sim L^{2.9}$, but somewhat smaller than the predicted value $\zeta = 6 - \bar{\eta} - \eta \approx 4.4$ [9]. We attribute this difference in ζ to the number of samples being too small to catch a sufficient number of rare samples which dominate the higher moments.

To conclude, while the data for the magnetization and disconnected susceptibility indicate a first order transition fairly convincingly, the specific heat seems to saturate to a finite value so there is no detectable latent heat. It is interesting to ask if the order of the transition might be different for a different random field distribution, since mean field theory predicts [14] that the transition becomes first order for large fields for the $\pm h$ distribution, but not, for example, for the Gaussian distribution. Since the multi-spin coding technique that we used does not work for a continuous distribution of fields, the answer to this question needs an even larger computing effort. Nevertheless we are currently attempting to carry out similar calculations for the Gaussian distribution. Our results are consistent with the Schwartz-Soffer inequality, Eq. (7), being satisfied as an equality, and support the scaling relation, Eq. (6). The scaling relation involving the specific heat, Eq. (8), does not seem to be satisfied, though our values for α may only be effective exponents particularly since we find α is negative and so a more detailed determination of non-singular background terms might be necessary to determine α accurately. Our results do support the prediction of the droplet theory that there are large sample to sample variations in the susceptibility at T_c .

We would like to thank D. P. Belanger for helpful discussions. One of the authors (HR) would like to thank the HLRZ at the KFA Jülich (Germany) for allocation of computer

time for the $L = 24$ run and acknowledges financial support from the DFG (Deutsche Forschungsgemeinschaft). The work of APY was supported in part by the NSF grant no. DMR-91-11576.

REFERENCES

- [1] For a recent review see T. Nattermann and J. Villain, *Phase Transitions* **11**, 817 (1988) and D. P. Belanger and A. P. Young, *J. Magn. Magn. Mat.* **100**, 272 (1991).
- [2] A. P. Young and M. Nauenberg, *Phys. Rev. Lett.* **54**, 2429 (1985).
- [3] A. T. Ogielski and D. A. Huse, *Phys. Rev. Lett.* **56**, 1298 (1986).
- [4] A. T. Ogielski, *Phys. Rev. Lett.* **57**, 1251 (1986).
- [5] J. Villain, *J. Physique* **46**, 1843 (1985).
- [6] D. S. Fisher, *Phys. Rev. Lett.* **56**, 416 (1986).
- [7] A. J. Bray and M. A. Moore, *J. Phys. C* **18**, L927 (1985).
- [8] D. P. Belanger, A. R. King, V. Jaccarino and J. L. Cardy, *Phys. Rev. B* **28**, 2522 (1983).
- [9] I. Dayan, M. Schwartz and A. P. Young, to be published.
- [10] H. Rieger, *J. Stat. Phys.* **70**, 1063 (1993).
- [11] D. Stauffer, C. Hartzstein, A. Aharony and K. Binder, *Z. Phys. B* **55**, 325 (1984).
- [12] M. Schwartz and A. Soffer, *Phys. Rev. Lett.* **55**, 2499 (1985).
- [13] M. Nauenberg and B. Nienhuis, *Phys. Rev. Lett.* **33**, 944 (1974).
- [14] A. Aharony, *Phys. Rev. B* **18**, 3318 (1978).

FIGURES

FIG. 1. The results of least square fits to data obtained by the procedure described in the text for $h_r/T = 0.35$. The points indicated by diamonds (\diamond) correspond to lattice sizes $L=4, 6, 8, 10, 12, 16$ — from right to left in (a) and (b) and left to right in (c) and (d). With the exception of the susceptibility we also inserted data for $L = 24$ with squares (\square), which we obtained by using a the same algorithm but on a CRAY Y-MP instead of the transputer array and which are averaged over only 64 samples. The $L = 24$ data were not used for the least square fits. (a) The temperature $T^*(L)$ of the specific heat maximum versus $L^{-1/\nu}$ with $\nu = 1.64$ and $T_c = 3.552$, see Eq. (5). (b) Specific heat $[C^*]_{\text{av}} \equiv L^{\alpha/\nu} \tilde{C}(x^*)$ versus $L^{-1/\nu}$ with $\alpha = 1.04$ and ν as in (a), see Eqs. (4) and (5). The specific heat appears to saturate for $L \rightarrow \infty$ at a value of $\lim_{L \rightarrow \infty} [C^*]_{\text{av}} \simeq 25.3$. (c) Susceptibility $[\chi^*]_{\text{av}} \equiv L^{2-\eta} \tilde{\chi}(x^*)$ in a log-log plot. The slope of the straight line is $2 - \eta$ with $\eta = 0.53$. The inset shows the second moment $[\chi^{*2}]_{\text{av}}$ of the probability distribution $P(\chi)$ in a log-log plot. The slope of the straight line is $\zeta = 3.82$. (d) Disconnected susceptibility $[\chi_{\text{dis}}^*]_{\text{av}} \equiv L^{4-\bar{\eta}} \tilde{\chi}_{\text{dis}}(x^*)$ in a log-log plot. The slope is $4 - \bar{\eta}$ with $\bar{\eta} = 1.0$. The insert shows the magnetization $[m^*]_{\text{av}} \equiv L^{-\beta/\nu} \tilde{m}(x^*)$ as a function of a L (the scale of the x-axis is logarithmic). The straight line is the extrapolation to $[m^*]_{\text{av}}(L = \infty)$, which is clearly nonzero and so $\beta = 0$.

FIG. 2. The histograms for the probability distribution $P(\chi)$ of the susceptibility for different $L = 8$ and 16 with $h_r/T = 0.35$. The temperatures are chosen to be as close to $T^*(L)$ as possible: $T = 3.80$ for $L=8$ and $T = 3.75$ for $L=16$.

The y-axes of the inserts are scaled differently to emphasize the long tail of the distribution. This feature originates in the rare samples with the extremely large values of the susceptibility scaling with the volume of the system (since $4 - \bar{\eta} \approx 3$).

TABLES

TABLE I. The critical exponents obtained via finite size scaling according to the procedure described in the text.

h_r/T	0.25		0.35		0.5	
T_c	3.9	± 0.1	3.55	± 0.05	3.05	± 0.05
ν	} $\frac{\alpha}{\nu} = -0.50$	± 0.05	1.6	± 0.3	1.4	± 0.2
α			-1.0	± 0.3	-1.5	± 0.3
η	0.60	± 0.03	0.56	± 0.03	0.6	± 0.1
$\bar{\eta}$	0.97	± 0.08	1.00	± 0.06	1.04	± 0.08
$\theta = 2 - \bar{\eta} + \eta$	1.6	± 0.1	1.6	± 0.1	1.6	± 0.1
β	0		0		0	
$(d - 4 + \bar{\eta})\nu/2$	0	± 0.05	0	± 0.05	0	± 0.05
$(d - \theta)\nu$			2.3	± 0.5	2.0	± 0.6
$2 - \alpha$			3.0	± 0.3	3.5	± 0.3

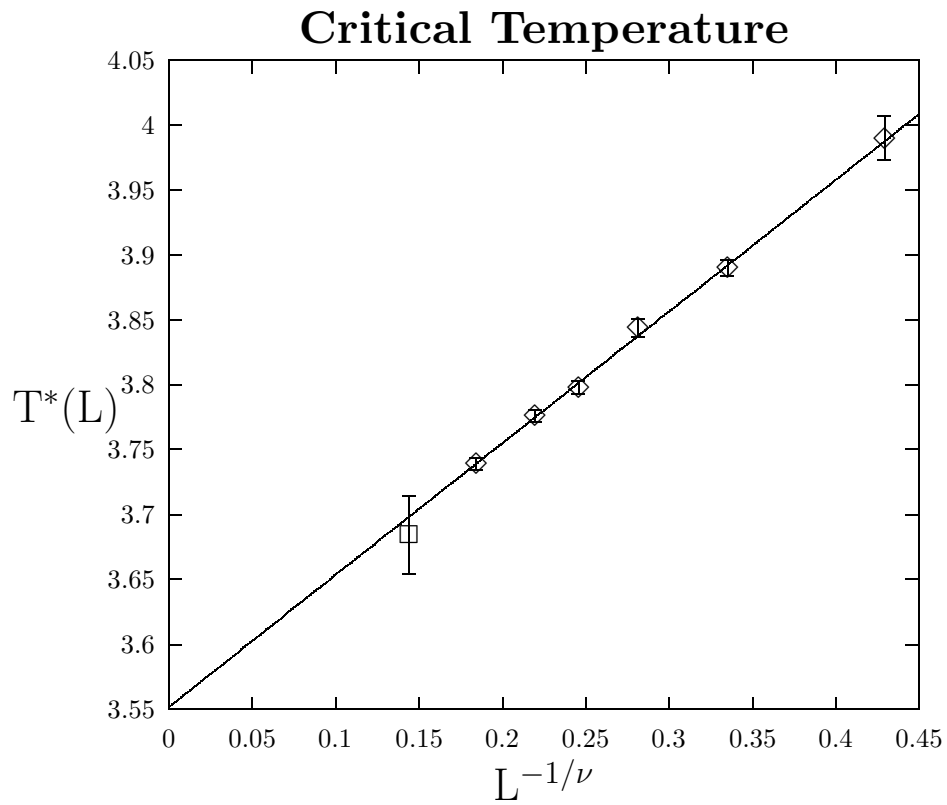


Fig. 1a

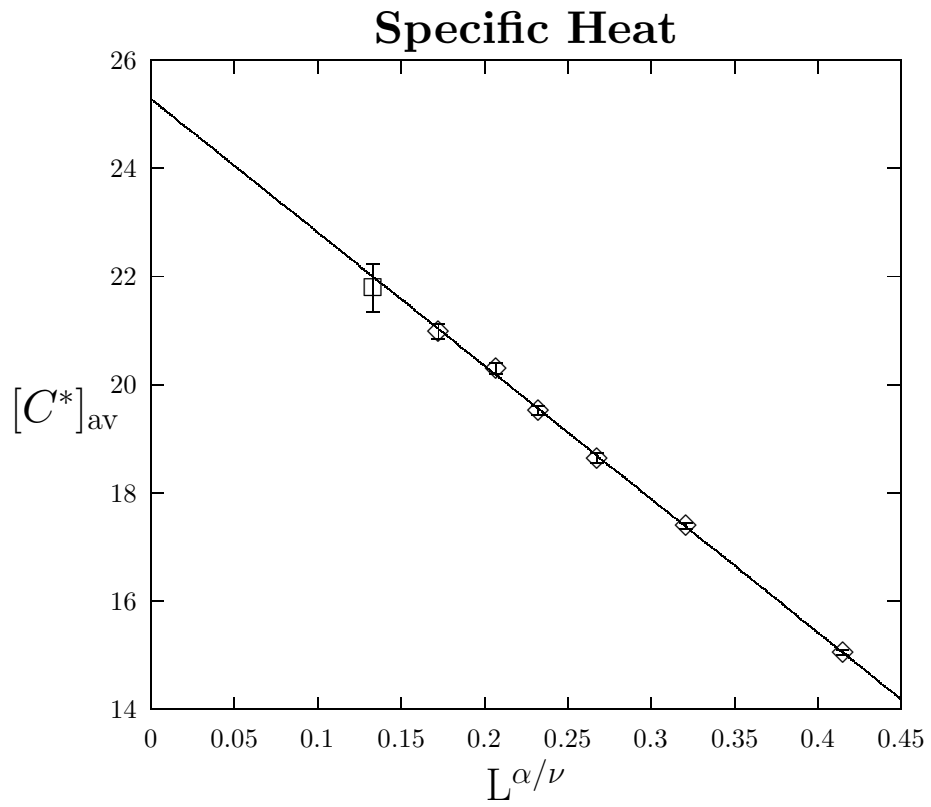


Fig. 1b

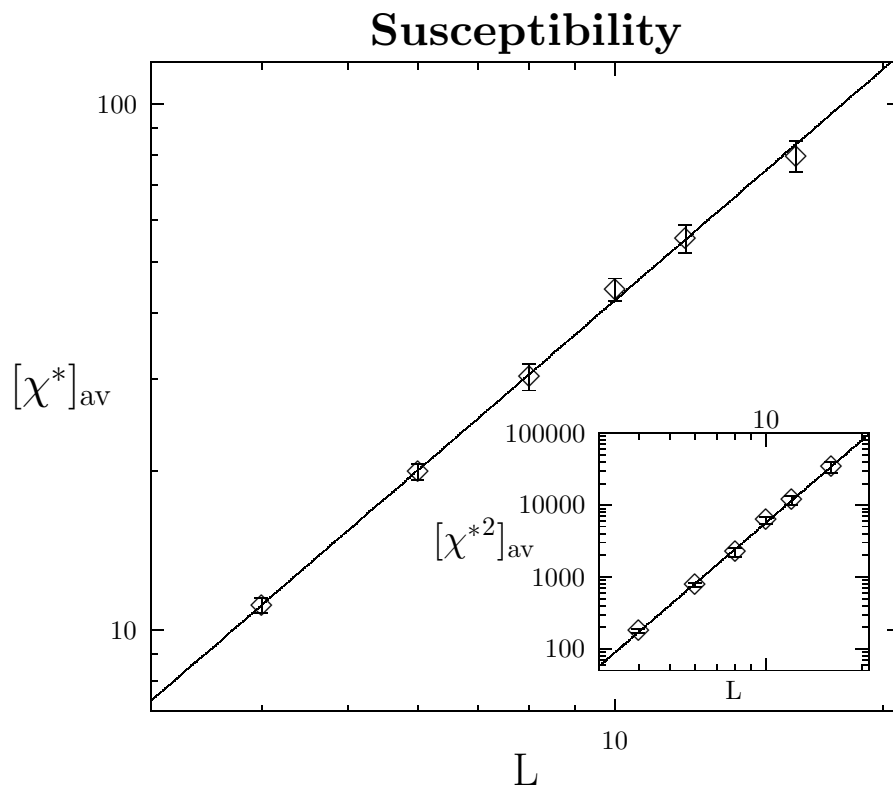


Fig. 1c

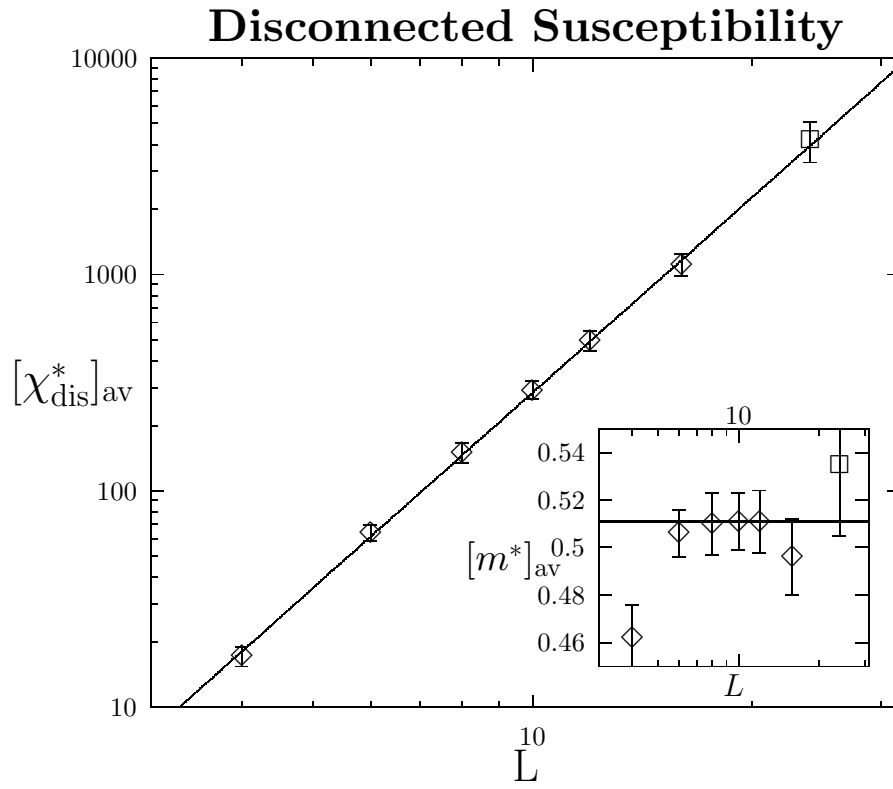


Fig. 1d